Direct Computation of Zero-Net-Mass-Flux Synthetic Jets

DECLAN HAYES-McCOY, XI JIANG
School of Engineering and Design
Brunel University
Uxbridge UB8 3PH
ENGLAND

DUNCAN LOCKERBY
School of Engineering
University Warwick
Coventry CV4 7AL
ENGLAND

Abstract: Axisymmetric direct numerical simulations (DNS) are performed to study the formation criterion and evolution of zero net mass-flux synthetic jets. Jet formation is defined by an oscillating streamwise jet centreline velocity, showing net momentum flux away from the orifice. This momentum flux away from the orifice takes the form of a series of vortical structures, often referred to as a vortex train. Modelling of the jet actuator consists of a modified oscillating velocity profile applied to a wall boundary. The jet issues into quiescent air, and the Reynolds numbers used vary from $85 < Re < 1000$. Variations to the input simulation parameters are carried out in order to determine the overall effects on the flow field. From these results the conditions necessary for the formation of the synthetic jet along with the input parameters that provide an optimal jet output are deduced. Jet optimisation is defined by both the vortical strength and longevity of the vortex train as it travels downstream. This study examines both the vortical structures, the jet centreline velocities along with other external flow characteristics in order to deduce and visualise the effects of the input parameters on the jet performance. The results attained on altering the oscillation amplitude and frequency of the jet actuator are in good agreement with previous studies. Further details on the jet centreline velocity for all cases are also presented; along with a study on the effects on the vortical structures of altering the Reynolds number of the flow.

Key-Words: Synthetic jet, DNS, axisymmetric, vortical structures

1 Introduction

The ability of jet actuators to alter turbulence production levels and thereby control the turbulence across an aerodynamic surface yields the possibility of skin-friction drag reduction for aerodynamic applications. The successful use of synthetic jet actuators for external flow applications suggests that there are potential aerodynamic gains to be achieved through the use of these devices in a number of internal flow regions, such as ducts and diffusers. Previous experimentation has largely ignored these internal flow applications.

Serpentine engine inlet ducts with a diffuser section introduce significant levels of distortion to the flow into the compressor. Active control of a synthetic jet actuator array could be used to reduce this distortion, mitigate associated unsteadiness, and improve the pressure recovery of the diffuser. Amitay & Pitt [1] carried out work into separation control and reattachment in diffusers using synthetic jet actuators, with positive results. This also suggests a possible further role for synthetic jet actuators in reducing the need for larger scale internal flow control devices, such as turning vanes.

This report computationally analyses the benefits to flow control that can be attained through the use of synthetic jet actuators. The direct numerical simulation (DNS) method used in the analysis allows an accurate capturing of the flow unsteadiness, which is the dominant characteristic of synthetic jets.

2 Synthetic Jet Actuators

Synthetic jet is a zero mass flux device, adding net momentum flux, but no mass flux to its surroundings. Jet formation is defined by Uttukar *et*

al. [2] as a mean outward velocity along the jet axis and corresponds to the clear formation of shed vortices. The layer of vorticity produced by the actuator rolls up to form a vortex ring under its own momentum. The momentum flux away from the orifice is actually a train of vortex rings or vortex pairs being dispersed from the diaphragm during the compression stroke. A pair of these vortices can be seen parallel to each other on either side of the orifice; each equal in magnitude but opposite in direction. Under certain operating conditions a vortex pair (vortex ring in the axisymmetric case) is formed at the orifice edge during the expulsion part of the cycle. This vortex pair is convected away from the orifice.

If the self induced velocity is strong enough, this vortex pair is not ingested back into the orifice on the suction part of the cycle. The strength of each vortex shed has been shown by Didden [3] to be related to the flux of vorticity through a (x, y) planar slice of the orifice during the ejection phase of the cycle. Holman & Utturkar [4] determined that jet formation is directly related to the flux of the vorticity from the synthetic jet. The breakdown of the turbulent jet flow tends to occur due to spanwise instabilities of the vortex pairs.

Depending on the flow symmetry and the repetition rate, the dynamics and interactions of the vortical structures within the pulsed jet can lead to spatial evolution that is remarkably different from the evolution of a continuous jet having the same orifice and time averaged flux of streamwise momentum.

Owing to the suction flow, the time averaged static pressure near the exit plane of a synthetic jet is typically lower than the ambient pressure, and both the streamwise and cross-streamwise velocity components reverse their direction during the actuation cycle. Smith and Glezer [5] defined the time periodic reversal of the flow leads to the formation of a stagnation point on the centreline downstream of the orifice and confines suction flow to a narrow domain near the exit plane.

3 Numerical Methods

Due to the intrinsic unsteady features associated with synthetic jets, typical Reynolds-averaged Navier-Stokes (RANS) methods do not provide sufficient detail to accurately predict the flow and accurately model the vortical structures present. This is due to the inherent time or ensemble averaging of the governing equations by RANS techniques. For this reason DNS is used in this case to resolve all the length and time scales therefore accurately predicting the vortical structures produced by the synthetic jet.

The highly accurate methods in DNS can yield both spatially and temporarily resolved solutions to the Navier-Stokes equations, thus accurately predicting the organised unsteadiness and vortical structures present in the flow. As the motivation behind this study is to determine the interaction of the vortical structures produced by a synthetic jet on the onset of turbulence, the accurate flow predictions by a DNS simulation are necessary.

The DNS code used for this work has a sixth-order numerical accuracy for the spatial differentiation and third order accuracy for the time advancement [6]. Compared with existing numerical studies, the highly accurate methods employed in this study will be able to more accurately resolve the unsteady vortical structures associated with the flow, which play a predominant role in the turbulence production cycle.

In this study the physical problem considered is a synthetic jet issuing into a wall-bounded domain. The mathematical formulation of the physical problem includes the governing equations for the synthetic jet and the highly accurate numerical solution methods employed to solve the fundamental governing equations, which are described previously [6]. The flow field is described with the compressible time-dependent Navier-Stokes equations for the axisymmetric jet. The nondimensional form of the governing equations is used. Major reference quantities used in the normalisation are the maximum centreline streamwise velocity at the jet nozzle exit (domain inlet), jet radius, density and viscosity.

The DNS numerical scheme [6] uses high-order finite difference schemes for the time advancement and spatial discretisation. The time-dependent governing equations are integrated forward in time using a fully explicit low-storage Runge-Kutta scheme. Spatial differentiation is performed by using the high order compact (Páde) finite difference scheme, which is sixth order at its inner points. The points next to the boundary are fourth order and the boundary points themselves are third order, thus the scheme has become known as the Páde 3/4/6 scheme. By applying symmetric conditions to both the primitive variables and their first and second derivatives in the radial direction, the Páde scheme has been extended to achieve the formal sixth order accuracy at the jet centreline, which is the boundary of the computational domain.

In the Páde 3/4/6 scheme, the formal sixth order accuracy at the inner points and symmetry boundary

is achieved by a compact finite difference differencing. Solutions for the discretised equations are obtained by solving the tridiagonal system of equations.

There are four boundaries to the computational domain [r: 0-Lr, x: 0-Lx], which represent half of the cross-section of an axisymmetric jet. These are: (1) the symmetric boundary at the jet centreline r=0. (2) The far side wall boundary in the radial direction r=Lr; (3) an inflow boundary at the domain inlet x=0, and (4) the wall boundary at the downstream location x=Lx. At the centreline the symmetry conditions are applied. Wall boundary conditions based on the Navier-Stokes characteristic boundary condition formulation [7] are applied at the side boundary in the radial direction and the streamwise directions.

4 Jet Simulations

4.1 Simulation details

Several computational cases have been examined; both to determine the simulation parameters required to achieve accurate results and to optimise the jet formation criterion.

Grid refinement studies were carried out, the results of which showed that accurate prediction of the vortical structures required a grid with a total cell count of over 1,000,000. The grid has a uniform distribution in the streamwise direction; however the cell size is sufficiently reduced near the jet shear layer in the radial direction.

As defined by the Courant-Friedrichs-Levy (CFL) condition, in a time-marching simulation the time step must be less than a certain criterion for stability and accuracy considerations. Therefore the CFL number must be sufficiently small to fully resolve the flow features for all actuator frequencies used. In practice the step used should be about one fortieth of the period of the main flow instabilities. In this study, tests with different CFL numbers have been performed and the final CFL number adopted ensures the results are time step independent.

The jet issues into a fixed domain nondimensionalised by radius of the jet orifice. The extent of the computational domain used is: Lx = 60, Lr = 6.

4.2 Effects of oscillation amplitude and frequency

For different pulsating frequencies and amplitudes applied at the inflow, the axisymmetric jet displays significantly different vortical flow structures. The effect of oscillation amplitude on the synthetic jets was found to be similar to that observed for nonzero-net-mass-flux pulsating jets. It was observed that the size of the jet potential core increases as the amplitude decreases. This is because jet mixing with ambient fluid decreases at smaller pulsating amplitudes. Vortices become larger downstream with smaller pulsating amplitudes; this is due to vortex merging occurring near the end of the jet potential core. For a perturbed jet with the frequency of perturbation within the range of jet preferred mode instability, the shear layer can roll-up and undergo successive interactions such as pairing and tearing through which the flow achieves gradual independence from the initial condition.

As stated by Jiang et al. [6], there is an optimum frequency at which an axisymmetric disturbance receives maximum amplifications in the jet column. Depending on the flow conditions, the optimum modes corresponds to a Strouhal number (nondimensional frequency) in the range St = 0.3 - 0.5, with the most commonly reported number being 0.3, where the Strouhal number is based on the jet diameter. Since the reference length scale in this study is the jet radius, the jet optimum mode should correspond to a frequency range of St = 0.15 – 0.25. Table 1 gives an outline of all the actuation frequencies analysed in this study. The Reynolds number used in the simulations was Re= 500.

Table 1. The computational cases

Designator	Actuator frequency
Case A: ———	f = 0.02
Case B: ---------	f = 0.04
Case C: —·—·—	f = 0.08
Case D: ·····	f = 0.16
Case E: —··—··—	f = 0.40

Figures 1 and 2 show the effect of oscillation frequency on the instantaneous flow characteristics of the zero-net-mass-flux synthetic jets. In Fig. 1, the line styles used for different computational cases correspond to those described in Table 1. It was seen in the results that larger pulsating frequency leads to smaller scale vortical structures and a corresponding reduction in the streamwise distance between vortical cores. At higher pulsating frequencies a further reduction in the vortex size occurs, resulting in the rapid deterioration of the vortical structures as they move downstream. This was indeed the case for the simulation with a nondimensional pulsating frequency of f = 0.40, which has no discernable vortical development downstream.

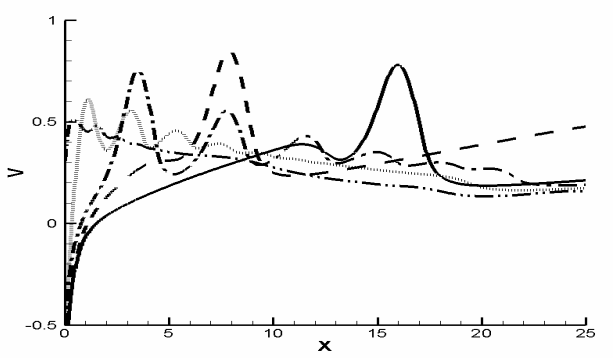

Fig. 1. Jet centreline velocities at t = 80.

For the formation of synthetic jets, an optimised case may be considered as associated with flow conditions under which the jet attains maximum longevity of vortical structures because vortical structures dominant the mixing and momentum transportation. The centreline streamwise velocity as shown in Fig. 1 of an optimised case should form a gradually decreasing oscillation away from the jet orifice. In the case with the nondimensional jet frequency of 0.4, no oscillation in the centreline velocity is present. This is due to re-ingestion of the expelled flow on the return stroke of the jet actuator, before it has travelled a sufficient distance downstream to remain unaffected. In this case the centreline velocity can be noted to drop quickly away from the orifice, with almost no trace of the previous velocity slug remaining.

Figure 2 shows the instantaneous vorticity contours at t = 80 of four computational cases. In this study, the low frequency cases (f = 0.02 & f = 0.04) do not exhibit true "jet like" characteristics as the oscillation frequency is below the level required to form a vortex train. In these cases only a single vortex pair is visible in the flow field; the vortices produced by previous actuator oscillation having completely deteriorated as the actuator completes its successive cycle.

The cases with the actuator frequency of f = 0.08 & f = 0.16 are the only two cases in this study in which a true jet stream with continuous vortical structures is created. It can also be noted that the velocity oscillations for the f = 0.16 case are lower in amplitude and decay more rapidly than the f = 0.08 case. This is assumed to be due to partial re-ingestion of the velocity slug with the higher actuator frequency. For the case with f = 0.16, at a location just beyond x = 10 the streamwise oscillation can be seen to be completely damped out.

The effect of the increased oscillation frequency is evident in Figs. 1 and 2. The only vortical structures present in the two low frequency cases (f=0.02 & f=0.04) are produced by the previous actuator oscillation. Although the vortical structures of a greater size than those produced by an actuator operating on a higher frequency, the vortical structures do not form a true jet flow. A 'train' of vortical structures can be seen moving downstream in both the f = 0.08 and f = 0.16 cases. However these vortical structures can be seen to degrade and finally disappear by x = 15 for the case with f = 0.08. The lack of any large scale vortical structures can also clearly be noted for the f = 0.4 case.

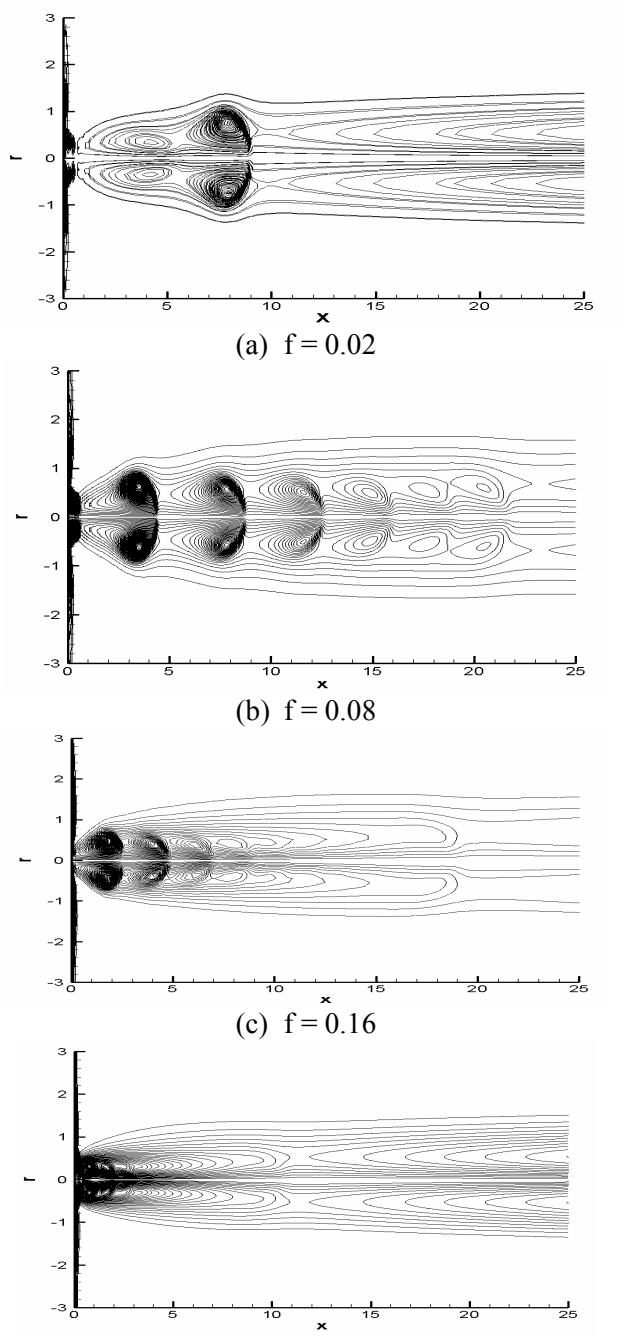

(a) f = 0.02

(b) f = 0.08

(c) f = 0.16

(d) f = 0.40

Fig. 2. Instantaneous vorticity contours at t = 80.

4.3 Effect of Reynolds number

As Reynolds number increases, smaller and smaller scales of the flow are visible. In the larger Reynolds number cases, there is not as much viscous effect present in the flow to dissipate the motions of the small scale eddies. Kinetic energy 'cascades' from large scale eddies to progressively smaller scales until a level is reached for which the scale is small enough for viscous forces become of the order of inertial ones. It is at these small scales where the dissipation of energy by viscous action predominantly takes place.

Experimentation with varying Reynolds number has a number of implications for determining both the Reynolds number range in which the simulation is valid and the optimum value with respect to maximising vorticity flux. As the Reynolds number decreases, the number of grid points required to achieve converged and grid-independent results decreases. Fig. 3 shows the instantaneous vorticity contours at t = 80 at two different Reynolds numbers. In Fig. 3, it can be seen that an increase in Reynolds number leads to an increased intensity and longevity of the vortical structures as they move downstream.

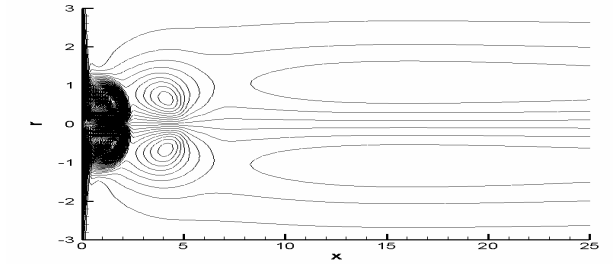

(a) Re = 85

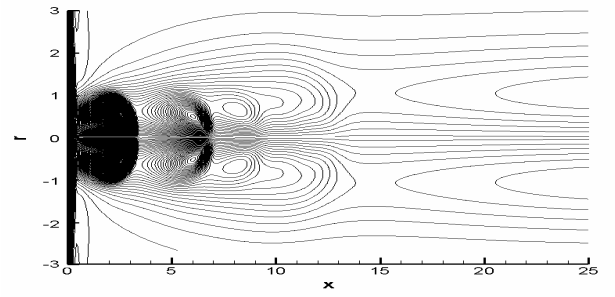

(b) Re = 165

Fig. 3. Effect of Reynolds number.

4.4 Jet optimised case

The insights into the effects of the input parameters on the production of a true jet flow were used to create an optimum case in terms of maximum longevity and vortical strength. Thereby increasing the turbulent kinetic energy of the flow field, and as shown by Dandois *et al.* [8], yielding the possibility of separation control and prevention. The parameters used are shown in Table 2. The vortical structures in this case can be seen to gradually reduce in magnitude as they move downstream. It can also be noted that, as the vortex convection speed associated with the streamwise mean velocity only decays slightly downstream; the distance between subsequent vortex centroids does not change significantly.

Table 2. Input parameters for the jet optimised case

Jet frequency	0.08
Domain extent (Lx, Lr)	60, 6
Number of cells	1,000,000
Reynolds number	300

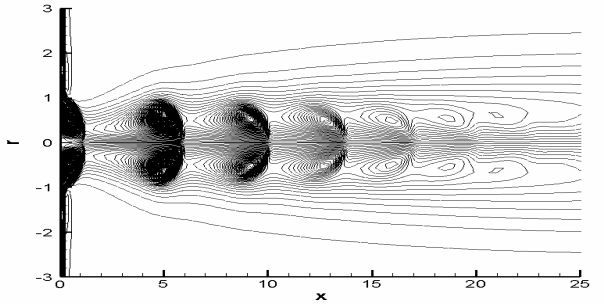

Fig. 4. Jet optimised case at t = 160.

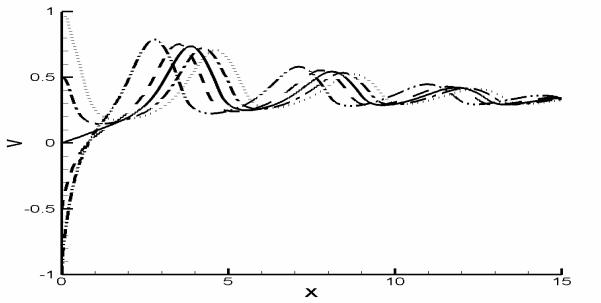

Fig. 5. Jet centreline velocity for one actuator cycle.

Table 3. Velocity profiles for one actuation cycle

Designator	Time instant
—·—·—	t = 150
---------	t = 152
———	t = 153
—·—·—·	t = 154
·····	t = 156

Figure 4 shows the instantaneous vorticity contours of the optimised case at t=160. Close comparisons can be made with Fig. 2(b), which uses the same input parameters, but simulated to t=80. It can be seen that there is no further progression of the vortical structures downstream during the time progression from t=80-160. Fig. 5 shows the jet centreline velocity within one actuator cycle of the optimised case, where the line styles used to

represent different time instants are described in Table 3. The flow unsteady behaviour is evident in Fig. 5, where the flow changes significantly at locations near the jet nozzle exit but less significantly at the downstream locations.

5 Conclusions

The optimisation of various input parameters of an axisymmetric synthetic jet actuator has been carried out. A highly accurate direct numerical simulation based upon the Páde scheme has been used to compute the vortical structures produced due to an oscillating velocity input applied at the jet orifice. The results attained have allowed a number of assertions to be made about the input characteristics which yield the optimum streamwise vortex train in terms of vortical strength and longevity.

Throughout the range of experimental cases examined various vortical structures have been observed in the flow field. The input parameter which was noted to have the greatest effect on jet formation was the actuator oscillation frequency. At low actuation frequencies the vortical structures present in the flow field were noted to be of a larger size; however a true 'vortex train' was not produced as the vortical structures were noted to travel downstream in lone vortex pairs. At high frequencies the jet was noted to be under expanded, in the region near the actuator. In this case vortical structures in the flow field were less coherent and did not persist in the downstream region. As previously stated, this has been determined to be due to re-ingestion of the expelled fluid from the actuator on the subsequent suction stroke.

Investigation into the effect of varying the Reynolds number showed the propagation of the vortical structures further downstream with higher Reynolds numbers, as expected.

The overall flow optimisation problem has been simplified by simply modelling the jet orifice as a sinusoidal oscillating velocity input, instead of a full modelling of the entire synthetic jet cavity flow. This initial investigation also uses an axisymmetric case in place of a full three-dimensional direct numerical simulation. Due to the nature of the axisymmetric simulation, there is lack of three-dimensional vortex interaction. This has previously been determined to be due to an inability of an axisymmetric simulation such as this to predict the flow features present due to the small scales. These small scales are of increasing importance in the downstream region, hence the reduction in vortical strength in these regions in this study. However the results attained give a valuable insight into the formation criterion of the synthetic jet along with optimal values for the actuator design.

References:

[1] Amitay, D., Pitt, D., Kibens, V., Parekh, D., Glezer, A., *Control of Internal Flow Separation Using Synthetic Jet Actuators*, AIAA 2000-0903, 2000.

[2] Uttukar, Y., Holman, R., Mittal, B. Carroll, M. Sheplak, and L. Cattafesta, *A Jet Formation Criterion for Synthetic Jet Actuators*, AIAA 2003-0636, 2003.

[3] Didden, N., On the formation of vortex rings: rolling up and production of circulation, *Journal of Applied Mathematics and Physics,* vol. 30, Jan. 1979, pp. 101-116.

[4] Holman, R., Utturkar, Y., Formation criterion for synthetic jets, *AIAA Journal*, Vol. 43, No. 10, 2005, pp. 2110-2116.

[5] Smith, B. L., Glezer, A., Vectoring of adjacent synthetic jets, *AIAA Journal*, Vol. 43, No. 10. 2005, pp. 2117-2124.

[6] Jiang, X., Zhao, H., Cao, L., Direct computation of a heated axisymmetric pulsating jet, *Numerical heat transfer Part A*, Vol. 46, 2004, pp. 957-979.

[7] Poinsot, T. J., Lele, S. K., Boundary conditions for direct simulation of compressible viscous flows, *Journal of Computational Physics*, Vol. 101, 1992, pp. 104–129.

[8] Dandois, J., Garnier, E., Sagaut, P., Numerical simulation of active separation control by a synthetic jet, *Journal of Fluid Mechanics,* Vol. 574, 2007, pp 25-58